Distribution of Dissolved LMW Hydrocarbons in Bristol Bay, Alaska: Implications for Future Gas and Oil Development

27

Joel D. Cline

Pacific Marine Environmental Laboratory
Seattle, Washington

ABSTRACT

In September and October, 1975, and again in July, 1976, the distribution of dissolved low molecular weight hydrocarbons was determined in Bristol Bay, Alaska. The concentrations were relatively low compared to other Alaskan shelf areas and show a significant seasonal signature. Local production of methane is accelerated in summer as it is for the alkenes. The concentrations of ethane and ethene are in linear relation in summer, suggesting a common source or perhaps a common organic precursor. The distribution of methane is strongly coupled to circulation and, in particular, to the location of hydrographic fronts. In contrast, the alkenes appear to be regulated more by biological activity than circulation. In composition, LMW hydrocarbons arising from a thermogenic source can be readily distinguished from their biological equivalents on the basis of the relative concentrations of ethane and ethene. Elementary modeling of a line hydrocarbon source suggests that hydrocarbon trajectories could be traced for several hundred km, assuming a source concentration 100 times above ambient levels. Other model scenarios are also considered.

INTRODUCTION

The low molecular weight (LMW) alkanes (i.e., methane, ethane, propane, iso- and *n*-butanes) are abundant constituents of crude oil and natural gas (Clark and Brown 1977). As such, they may indicate the presence of crude oil and thermogenic gas in marine waters. These gases may originate in production activities associated with offshore drilling, venting, and transportation and transfer operations (Brooks and Sackett 1973 and 1977, Bernard et al. 1976), or they may arise from natural hydrocarbon seeps (Carlisle et al. 1975, Dunlap et al. 1960, Sackett 1977, Cline and Holmes 1977).

The LMW alkanes represent a significant fraction of many crude oils, and they also are produced in small but significant amounts in marine waters and sediments (Brooks and Sackett 1973, Swinnerton and Lamontagne 1974, Bernard et al. 1978). Methane, the most abundant LMW hydrocarbon, is produced through the fermentation of simple organic acids or in hydrogen reduction of CO_2 by anaerobic microorganisms (McCarty 1964, Wolfe 1971, Reeburgh and Heggie 1977). Recent evidence suggests that methane is also produced in oxic marine waters, presumably from organisms living in reducing microenvironments (Scranton and Brewer 1977).

On the other hand, the origin of the C_2-C_4 compounds is less clear. It is known, for example, that ethene is produced by soil bacteria (Smith and Cook 1974), but the significance of these organisms in ocean waters is not known. What is known, however, is that the alkenes ethene and propene are usually enriched in surface ocean waters (Swinnerton and Lamontagne 1974, Cline et al. 1978). Production of these compounds in marine surface waters appears to be a photochemical process involving dissolved organic carbon (Wilson et al. 1970), but a biological contribution from microorganisms cannot be completely dismissed on the basis of currently available data (Lamontagne et al. 1975).

The purpose of this chapter is to present the distributions and abundances of dissolved LMW hydrocarbons in Bristol Bay, Alaska. The study was carried out in September and October 1975 and July 1976. Emphasis is on the natural occurrences, their relationships to circulation and source regions, and the potential usefulness of these compounds in tracing both catastrophic and chronic petroleum contamination arising from future resource development. This program was developed in response to objectives set

forth in the Environmental Study Plan for the Gulf of Alaska, Southeastern Bering Sea, and the Beaufort Sea (DOI/DOC 1975).

SAMPLING AND CHROMATOGRAPHIC ANALYSIS

Water was collected in PVC Niskin® samplers attached to a Plessy model 9040 CTD-rosette system deployed at predetermined depths. Upon retrieval, water was carefully transferred to 1-liter glass-stoppered bottles so as not to include bubbles, allowing one volume to overflow for rinsing. To inhibit biological activity, 100-200 mg sodium azide was added to each sample. Samples were stored at ambient temperatures (approximately 5-10 C) in the dark until analyses could be accomplished, usually within two hours of sampling.

Dissolved low molecular weight hydrocarbons, C_1-C_4, were quantitatively removed from solution by a modification of a procedure originally proposed by Swinnerton and Linnenbom (1967). In the modified procedure, hydrocarbons were removed in a stream of helium (approximately 100 ml/min) and concentrated on a single Activated Alumina® trap (0.64 cm o.d. × 5 cm) held at −196 C (LN_2). Quantitative stripping of the hydrocarbons was achieved in 10 minutes at which time the trap was warmed to 100 C and the hydrocarbons injected into a gas chromatograph (Hewlett-Packard model 5711) equipped with dual flame ionization detectors. Chromatographic separation of the components was originally effected on a Poropak® Q column (0.48 cm o.d. × 2.5 m) held isothermally at 30 C. With a helium carrier flow rate of 60 ml/min, analysis was completed in 15 minutes. During the second cruise (July 1976), the chromatographic column was modified by adding a short activated alumina column (0.48 cm o.d. × 5 cm) impregnated with 1 percent silver nitrate by weight. This modification, coupled with temperature programming from 110 C to 150 C, resulted in sharper peaks, improved separation of the alkenes, and shorter analysis time (Cline and Feely 1976).

Calibration was carried out by injecting and trapping 1-ml volumes of a certified standard hydrocarbon mixture prepared by the Matheson Co. This standard mixture was subsequently recalibrated by NBS and found to conform to the previously stated accuracy of 10 percent for each component.

Replicate analyses of water samples were carried out at three stations in Bristol Bay during the fall cruise. A general analytical precision of 5 percent (relative std. dev.) was observed for the components methane, ethane, and ethene, whereas the remaining components were found in concentrations too low to provide meaningful estimates of precision. Subsequent measurements made in July 1976 show that precision for propane and propene was also near 5 percent; again butanes were present at or below their detection limit.

PHYSICAL SETTING AND HYDROGRAPHY

Bristol Bay is a broad shelf region located in the southeastern Bering Sea. It is bounded on the south by the Alaska Peninsula, on the west by the shelf break, and on the north by the Alaska Coast (Schumacher et al. 1979). Freshwater influx, originating primarily from the Kuskokwim and Kvichak watersheds, averages 47 km^3 annually (Kinder 1977). Ice covers approximately 60 percent of Bristol Bay between the months of December through April (Schumacher et al. 1979).

There are three principal water masses that have been identified in Bristol Bay (Coachman and Charnell 1977). The warmest and most saline water is found along the outer southern shelf (cf. Fig. 2, Coachman and Charnell 1977). Between this water mass and the 50-m isobath is the middle shelf water, which is usually stratified thermally in summer. Bottom temperatures of −1 C are not uncommon. The coastal water ($z < 50$ m) is characterized by the lowest salinity and may or may not be stratified, depending on the season, depth of water, and freshwater influx.

Currents over the shelf are generally weak (Kinder and Coachman 1978, Coachman and Charnell 1979). Along the outer shelf, in summer, current trajectories generally trend northwest at speeds of approximately 5 cm/sec. Across the inner shelf, currents are weak (~ 1 cm/sec) and variable.

Frontal structures have been observed along the 50-m and 100-m isobaths, which hydrographically separate the various water domains. Development of the front in shallow water appears to be related to the onset of stratification and tidal mixing (Schumacher et al. 1979).

RESULTS

Bristol Bay was sampled for dissolved LMW hydrocarbons in September and October 1975 and in June and July 1976. Vertical profiles were made at each of the stations shown in Fig. 27-1, although instrumental difficulties and weather forced curtailment of sampling at a few stations. To document temporal changes occurring over tidal frequencies, time-series

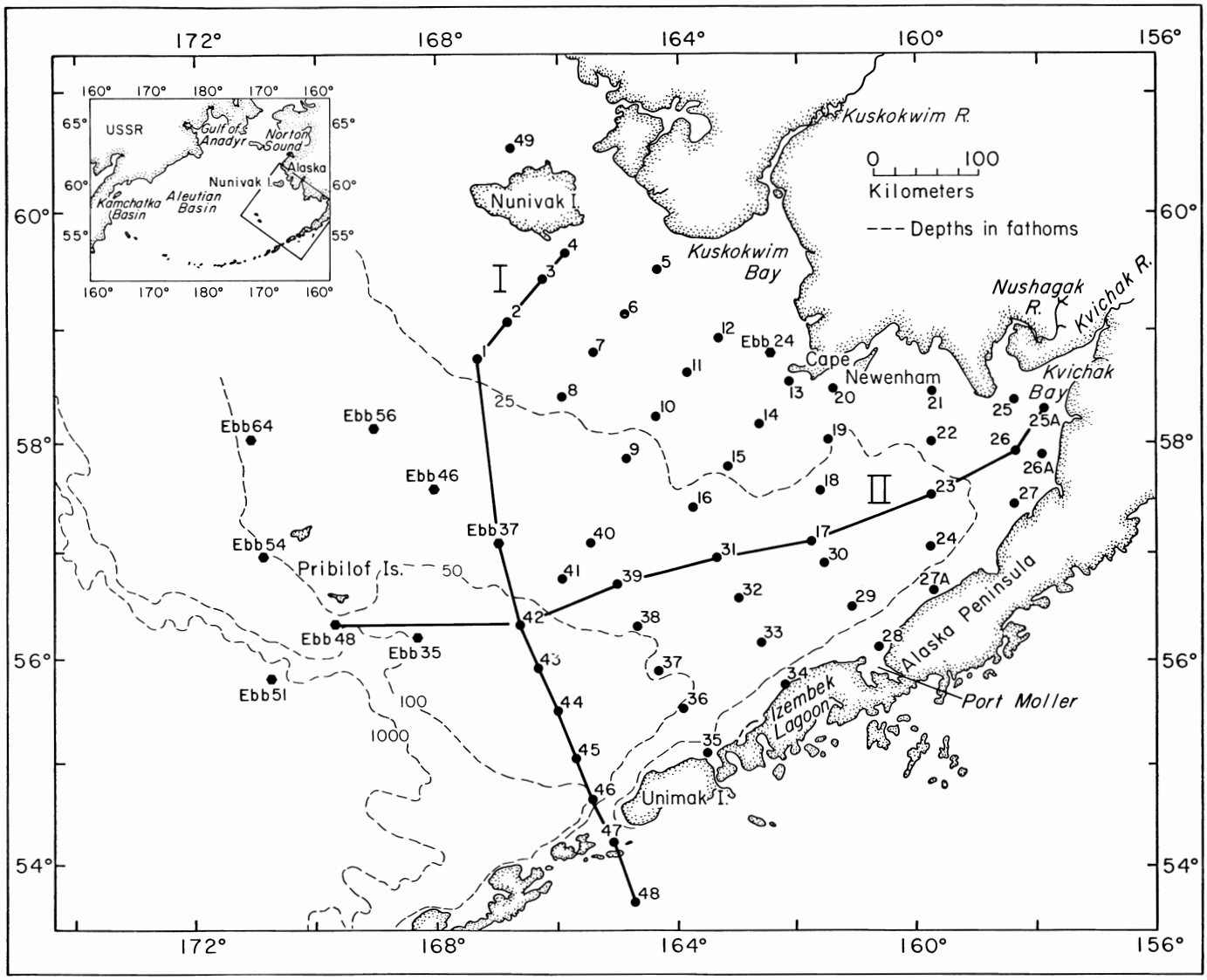

Figure 27-1. Location of stations occupied in Bristol Bay in Sept.-Oct. 1975 and July 1976. The solid lines show the vertical sections along which the distribution of properties is discussed. Depth contours are in fathoms.

measurements (24 hours and 36 hours) were made at Stations Ebb 37 and 46 in September and October, 1975. In addition to the sampling for dissolved hydrocarbons, measurements of salinity, temperature, and concentrations of suspended matter were also made at each of the stations shown (Feely and Cline 1977).

Methane

Methane is the dominant dissolved LMW hydrocarbon and its distribution reflects both seasonal and spatial source patterns. The distributions of dissolved methane in surface and near-bottom waters are shown in Figs. 27-2a and b for September and October 1975. Except for a localized source near Port Moller, surface concentrations of methane were near values expected from the saturation of air. Assuming a methane partial pressure of 1.4 ppm(v) (Ehhalt 1974) and a mean surface temperature and salinity of 7 C and 31°/oo (Kinder and Schumacher, Chapter 4, this volume), the equilibrium solubility concentration of CH_4 is 53 ± 3 nl/l (STP) (Yamamoto et al. 1976). The plume of methane observed south of Cape Newenham may have arisen from the Nushagak and Kvichak Rivers, although the small enrichment noted (75 nl/l < CH_4 < 94 nl/l) is near the ambient noise level when variability in time and space is taken into account. These data, however, do not rule out a contribution from bottom sediments in the Kuskokwim Delta.

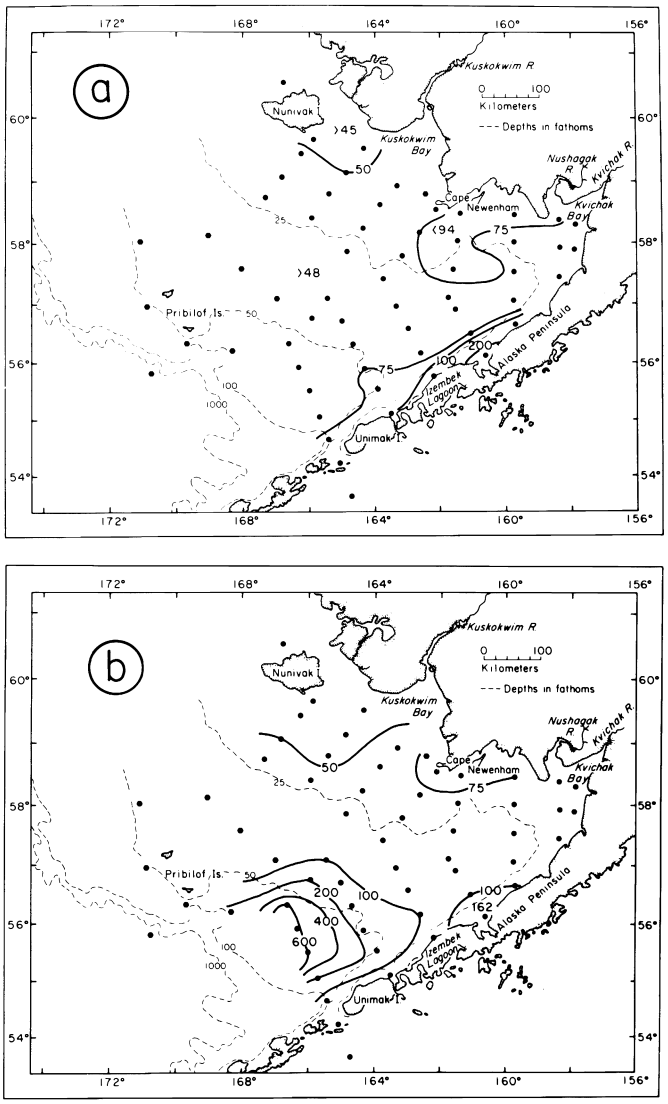

Figure 27-2. Surface (a) and near-bottom (b) distributions of dissolved methane (nl/l, STP) in Sept.-Oct. 1975. Near-bottom samples were taken within 5 m of the bottom.

The elevated concentrations near Port Moller presumably arise from the tidal discharge of methane-rich waters from the lagoon. It is interesting, however, that methane is contained inside the 50-m isobath. The lack of a definite plume trajectory either east or west also suggests that there was little or no persistent coastal current at the time of these measurements. This is in general agreement with circulation studies carried out in Bristol Bay over the past several years (Kinder and Schumacher, Chapter 5, this volume), in which wind forcing or other meteorological events may give rise to a coastal current. The strong lateral methane gradient in the absence of any significant mean flow also suggests that the previously described frontal system along the 50-m isobath (Schumacher et al. 1979) inhibits a horizontal flux of methane to the north.

The concentration of methane within 5 m of the bottom is shown in Fig. 27-2b. The most striking feature is the concentrated source over the outer shelf, referred to here as St. George Basin. Concentrations of methane near the bottom were in excess of 600 nl/l (STP) and represent approximately 12-fold supersaturation with respect to the atmosphere. The source of the methane is undoubtedly microbial, presumably arising from the activities of microorganisms at the sediment-water interface. According to Sharma (1979), bottom sediments along the outer shelf are fine grained, containing more than 0.5 percent organic carbon by weight. While these concentrations of carbon are not inordinately high, they are enriched compared to the inner shelf region, where concentrations range from 0.05 percent to 0.2 percent (Sharma 1979). The exception to this generalization is Kuskokwim Bay, where organic carbon concentrations range from 0.1 percent to 0.5 percent. These fine-grained sediments also are a likely source of methane, as mentioned earlier.

The methane distribution inside the 50-m isobath was vertically homogeneous. This distribution is expected if the bottom production rates are small compared to the rate of vertical mixing. Salt and heat were also vertically homogeneous in the coastal water, suggesting strong vertical mixing at the time of the measurements (Kinder and Schumacher, Chapter 4, this volume). For the sake of brevity, the distributions of salinity and temperature for that period will not be shown as they were similar to those observed by Schumacher et al. (1979) for the following year.

In Bristol Bay, the distribution of methane is controlled by several point sources and circulation. This is apparent in Fig. 27-3, where the vertical distribution of methane is shown along a north-south section between Nunivak Island and Unimak Pass (see Fig. 27-1; Sec. I). Methane in St. George Basin clearly originates from the bottom. While a weak mean current over the outer shelf (Kinder and Schumacher, Chapter 5, this volume) may transport methane to the northwest, this figure clearly shows the influence of vertical mixing on the distribution of methane. Because of increased vertical turbulence, methane-rich water was observed at the surface near Unimak Pass (Sta. 46). In contrast, the inner shelf region was nearly homogeneous with respect to dissolved methane, with concentrations near the equilibrium values.

In order to evaluate the short-term variability of methane, Stations 46 and Ebb 37 were sampled every 4 hours for 24 hours and 36 hours respectively. The results of the time-series measurements are

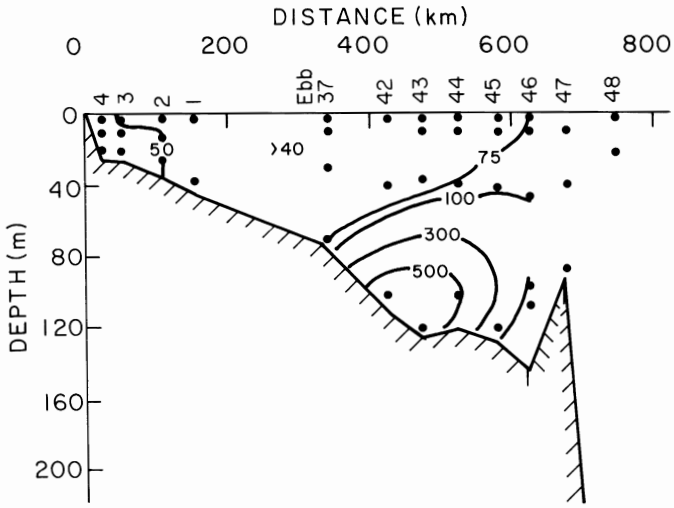

Figure 27-3. Dissolved methane (nl/l, STP) along a north-south section through Unimak Pass. Observations were made in Sept.-Oct. 1975.

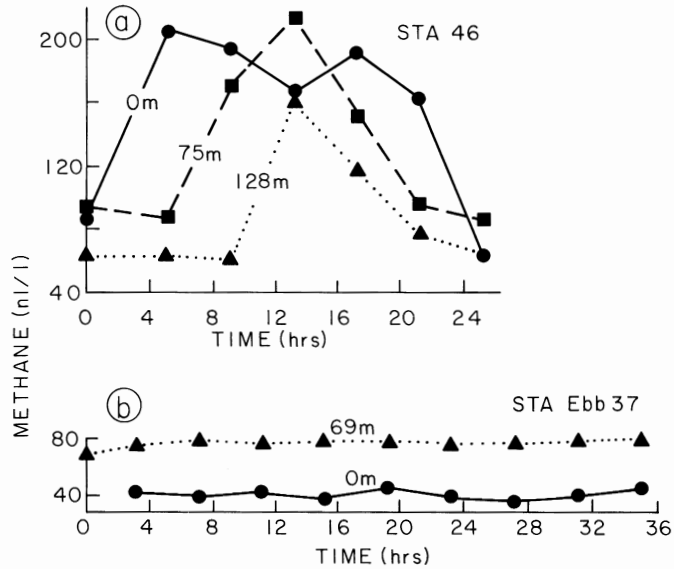

Figure 27-4. Short-term variability of dissolved methane at stations 46 (a) and Ebb 37 (b) in Sept.-Oct. 1975.

shown in Figs. 27-4a and b. At the beginning of the observations (Sta. 46), the distribution of methane was vertically homogeneous, or nearly so. At approximately 4 hours, methane concentration in the surface layers increased to over 200 nl/l and remained high for the following 20 hours. Similar trends were observed at depth although there appeared to be a significant lag period (four to five hours). Because the only reasonable source of the methane is St. George Basin, it is assumed that during the observational period water was advecting south through Unimak Pass.

To the north at Station Ebb 37, just east of the Pribilof Islands, the concentration of methane at the surface and at depth was uniform over the entire observational period. This suggests that methane-rich water from St. George Basin did not move onto the shelf during this period. On the contrary, the mean current trajectory was probably parallel to the isobaths and would result in advection of dissolved methane toward the northwest (Coachman and Charnell 1979).

In contrast to conditions observed the previous fall, concentrations of all LMW hydrocarbons were elevated in the surface waters during July. Concentration of dissolved methane in the surface waters is shown in Fig. 27-5a. Port Moller once again was a significant source, as it was the previous fall. A concentration of methane greater than 1300 nl/l was observed at Station 28, or a value approximately 26 times the saturation amount. The source of this methane is believed to be sediments rich in organic matter inside Port Moller, where decomposition of vegetable matter could result in the vigorous production of methane. In the absence of significant microbial oxidative processes, methane dissolved in the shallow brackish waters of the lagoon would be transported through the entrance by tidal pumping (Barsdate et al. 1974).

Because the air-sea exchange of methane is relatively slow, advection of methane-rich water could be traced east along the Alaska Peninsula for nearly 200 km. Although a cyclonic mean flow in the coastal water does not appear to dominate the shelf salt budget (Coachman and Charnell 1979), a weak coastal current exists along the peninsula (Kinder and Schumacher, Chapter 5, this volume).

The surface distribution of methane in July, not unlike temperature, delineates quite sharply the hydrographic domains over the shelf. Near the shore in water depths less than about 50 m, the concentrations of methane were everywhere greater than 100 nl/l and reflected increased production relative to the previous fall. The source of the methane is not known precisely, but would include coastal sources as well as *in-situ* production from both bottom sediments and the water column.

The Kuskokwim River may also be a significant source of methane as suggested by the high concentrations (> 400 nl/l) found near Cape Newenham. The Kuskokwim River was not sampled for dissolved hydrocarbons, but the Yukon River plume was sampled in July 1979 and found to contain concentrations of methane in excess of 2,000 nl/l. We would expect the lower reaches of the two rivers to be similar in dissolved methane content, since their lower drainage basins are similar. As mentioned

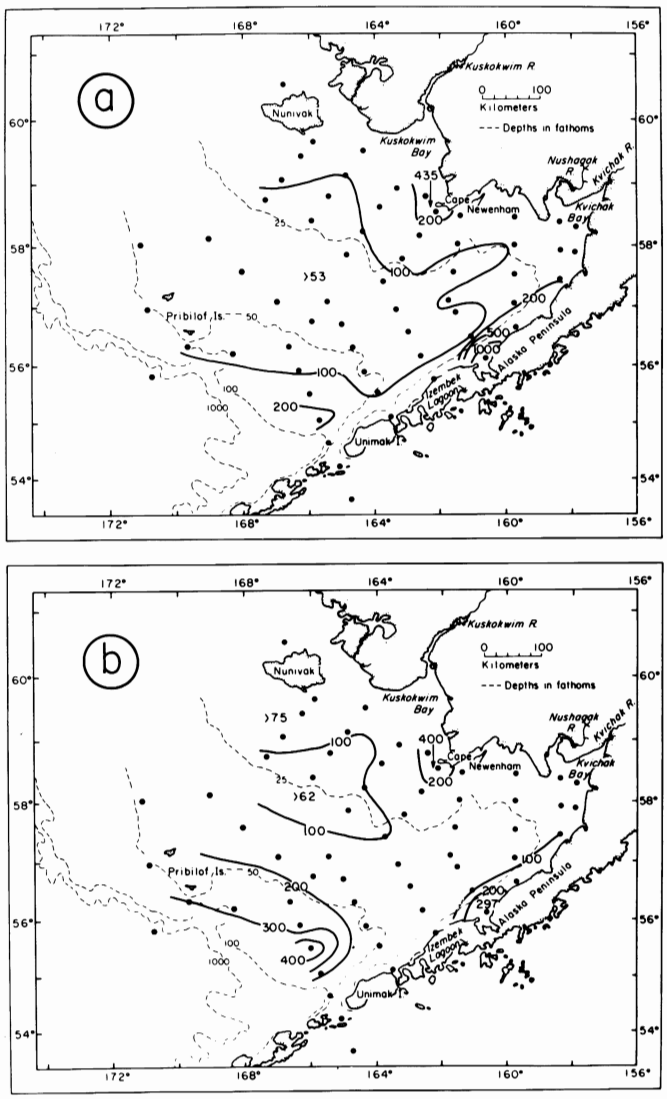

Figure 27-5. Surface (a) and near-bottom (b) distribution of dissolved methane (nl/l, STP) in July 1976. Near-bottom samples were taken within 5 m of the bottom.

above, however, the benthic production in Kuskokwim Bay must be considered on the basis of the available data.

Methane concentrations in the surface waters of the middle shelf during July ranged from 50-100 nl/l (Fig. 27-5a). Vertical stratification and low production of methane result in the observed distribution. The near-bottom distribution of methane is reflected in Fig. 27-5b. Previously identified sources near Port Moller and Cape Newenham are evident, although concentrations at depth are somewhat reduced. This observation would be expected if the rivers in the area are a significant source of the methane.

The bulk of the middle shelf water contained rather uniform levels of methane (50-100 nl/l), except for the outer shelf region north of Unimak Pass, where concentrations in excess of 400 nl/l were found. These concentrations are slightly less than the values observed the previous fall (see Fig. 27-2b) and suggest that methane production is seasonal. Water temperature, carbon production rate, and quality of the organic matter would all be expected to strongly influence the production rate of methane, hence the *in-situ* concentration., if dispersive factors remain constant.

The influence of circulation and mixing on the distribution of methane is depicted in Fig. 27-6a, a zonal section through Bristol Bay (see Fig. 27-1; Sec. II). Methane is vertically homogeneous in the coastal water (Sta. 25A-17), but shows vertical structure over the middle shelf (Sta. 17-42). Surface waters in the middle shelf region are close to saturation with respect to methane in the atmosphere, whereas

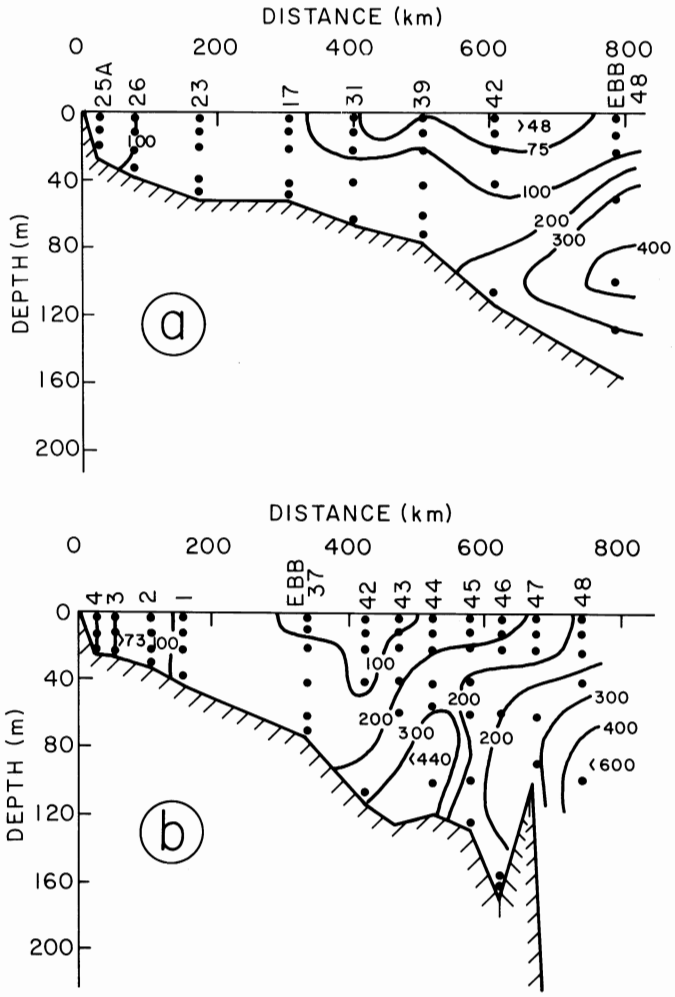

Figure 27-6. (a) Vertical distribution of dissolved methane (n/nl, STP) along Sec. II in Bristol Bay (see Fig. 27-1). (b) Vertical distribution of dissolved methane (nl/l, STP) along Sec. I terminating in Unimak Pass. Observations were made in July 1976.

concentrations increase to near 200 nl/l at depth. Analogous to the situation predicted for salt (Coachman and Charnell 1979), some of the methane found over the middle shelf probably originates by lateral diffusion from the outer shelf. Undoubtedly, there is an indigenous source, but its significance cannot be evaluated at this time.

A core of methane-rich water is evident at Station Ebb 48 (Fig. 27-6a). It presumably originates from the southeast in water depths near 120 m (see Fig. 27-6b; near Sta. 44). The core properties of the methane suggest a mean flow at depth toward the northwest. Current-meter observations of Kinder and Schumacher (Chapter 5, this volume) taken over the outer shelf for the period June-July 1976 show a net current speed of 1-2 cm/sec at 100 m to the northwest (see their Sta. BC-13B), supporting the observed methane trajectory.

The distribution of methane along a north-south section between Nunivak Island and Unimak Pass is shown in Fig. 27-6b. General structural features shown in Fig. 27-6a are preserved in this section, except for the complexity of multiple sources near Unimak Pass (Sta. 45-48). In contrast to the conditions observed in the previous year (see Fig. 27-3), there was a large accumulation of methane at depth south of Unimak Pass. The highest concentration of methane (630 nl/l) was observed at 400 m (Sta. 48), rather deep penetration for methane presumably originating from shallow shelf waters. However, since the concentration of methane at 100 m was 550 nl/l, methane-enriched water found offshore probably originated from the broad shelf along the southern Aleutian Peninsula. Whereas the data in Fig. 27-6b suggested a northward movement of water through Unimak Pass during the observational period, it probably was not sustained for any significant period of time. This is exemplified by our observations of methane in the vicinity of Unimak Pass during September and October 1975 (see Fig. 27-4a).

LMW hydrocarbons

The concentrations of the C_{2+} hydrocarbons (C_2 to C_4) are governed largely by seasonal processes involving biological activity or increased levels of insolation. Frontal dynamics appear to play a lesser role in controlling the distribution of these than for methane. A summary of the hydrocarbon concentrations (means and standard deviations) for the various hydrographic domains is shown in Table 27-1. For the purpose of clarity and to delineate possible source regions, the data were organized according to hydrographic domains as described by Coachman and Charnell (1977). Distinctions are also made between surface waters and near-bottom waters.

Because of analytical problems encountered during the fall cruise, the concentrations of ethene and propene include those of ethane and propane. Many observations conducted in the coastal waters of Alaska show that the concentration of ethene is approximately three times that of ethane (see Fig. 27-8). The relationship of propene and propane is similar.

Since concentrations of butanes (iso- and *n-)* were always below the detection threshold of 0.05 nl/l, they are not included in Table 27-1. They do, however, occur in measurable amounts near well-defined gas seeps in Norton Sound and Cook Inlet (Cline and Holmes 1977, Cline 1977).

Both ethene and propene show a significant seasonal signature in surface waters. For example, the surface distribution of ethene during the summer of 1976 is shown in Fig. 27-7. Localized sources of ethene are not well defined, although the eastern portion of Bristol Bay appeared to be more productive than the outer shelf region in July. The distribution of ethene, like methane, does not correlate well with the hydrographic parameters. The reason for this probably lies in the relative rates of production and the decoupling of ethene production from hydrographic domains: water-column production of ethene is not influenced strongly by the 50-m frontal system, but is largely controlled by photochemical and biochemical processes in the surface and near-bottom waters.

During the fall, in all hydrographic domains, the concentration of ethene was less than 1 nl/l, increasing to concentrations greater than 2 nl/l in summer. A similar trend was noted for propene, although the concentrations were systematically less.

As expected, the vertical distribution of the C_1-C_4 hydrocarbons in the coastal domain is invariant, although the seasonal component is evident in the depth-averaged mean concentrations (Table 27-1). This fact suggests that hydrocarbon production occurs in the water column or possibly at the sediment-water interface. If hydrocarbon production occurs principally at the sediment-water interface, tidally induced turbulence appears to be strong enough to homogenize the coastal water mass. A similar phenomenon obtains for heat and salt (Kinder and Schumacher, Chapter 4, this volume).

In the middle shelf domain ($50 \text{ m} < z < 100 \text{ m}$), the influence of both surface production and vertical stability come into play. Methane showed little seasonal difference (average), suggesting that water-column production was minimal and whatever vertical structure was present can be attributed to changes

TABLE 27-1

Average surface (a) and near-bottom (b) concentrations (nl/l, STP) of methane, ethane, ethene, propane, and propene for various water depth intervals.

CRUISE	DOMAIN		METHANE Mean	METHANE Range	ETHANE Mean	ETHANE Range	ETHENE[1] Mean	ETHENE[1] Range	PROPANE Mean	PROPANE Range	PROPENE[1] Mean	PROPENE[1] Range
	Coastal	a	64	45-94	--	--	0.9	0.3-17	--	--	0.5	0.2-11
	(<50 m)	b	59	45-98	--	--	1.0	0.7-1.8	--	--	0.4	0.1-0.6
Sept.-Oct.,	Middle Shelf	a	60	42-83	--	--	0.8	0.3-1.6	--	--	0.4	0.1-1.4
1975	(50-100 m)	b	99	65-163	--	--	1.7	1.2-2.7	--	--	0.6	0.3-1.3
	Outer Shelf	a	76	40-200	--	--	0.5	0.2-0.8	--	--	0.3	0.3-0.4
	(100-200 m)	b	380	100-615	--	--	1.1	0.7-1.6	--	--	0.3	0.2-0.4
	Coastal	a	112	74-153	0.9	0.6-1.5	3.8	3.0-4.7	0.4	0.3-0.6	1.4	1.0-2.5
	(<50 m)	b	114	73-153	1.0	0.5-2.5	3.4	2.3-4.4	0.4	0.2-0.6	1.2	0.7-1.6
June-July,	Middle Shelf	a	85	52-134	0.6	0.3-1.5	2.9	1.9-4.7	0.3	0.2-0.6	1.1	0.6-1.7
1976	(50-100 m)	b	115	62-165	1.3	0.5-2.5	2.2	1.1-4.0	0.5	0.3-0.6	0.5	0.2-1.0
	Outer Shelf	a	140	53-276	1.1	0.4-2.1	2.3	1.8-2.8	0.4	0.2-0.7	0.7	0.5-1.1
	(100-200 m)	b	269	164-440	0.9	0.6-1.1	1.2	0.8-1.8	0.3	0.2-0.4	0.3	0.1-0.9

[1] Due to analytical difficulties encountered during the Sept.-Oct. 1975 cruise, concentrations of ethene and propene include ethane and propane respectively.

in vertical stability. Because of vertical stratification, concentrations of methane below the thermocline are somewhat higher than in the surface layers, although not significantly so in the summer of 1976 (Table 27-1). This observation suggests a small benthic source.

In fall the highest concentration of ethene was found at depth, whereas in summer the concentration was higher in the surface layers. This difference is attributed to increased biological or induced photochemical production in the surface layers. Similar trends are apparent in the distribution of propene, but because of lower concentrations (i.e., lower production rate), seasonal and spatial variations are more obscure and probably not statistically significant.

The salient hydrocarbon features characteristic of the outer shelf domain (100 m < z < 200 m) were the high concentration of methane in the near-bottom waters and a relative increase in the concentration of ethane and propane compared to that of ethene and propene. The ethane/ethene ratio was significantly larger in the bottom waters of the outer domain than observed elsewhere in Bristol Bay. This relationship is attributed to the influence of organic-rich, possibly anoxic sediments near the sediment-water interface that modify the normal alkane/alkene ratio. For example, the dominant C_{2+} hydrocarbons in the anoxic waters of the Black Sea are the alkanes, indicating that the production of biological hydrocarbons under anoxic conditions tends toward the more reduced alkanes (Hunt 1974).

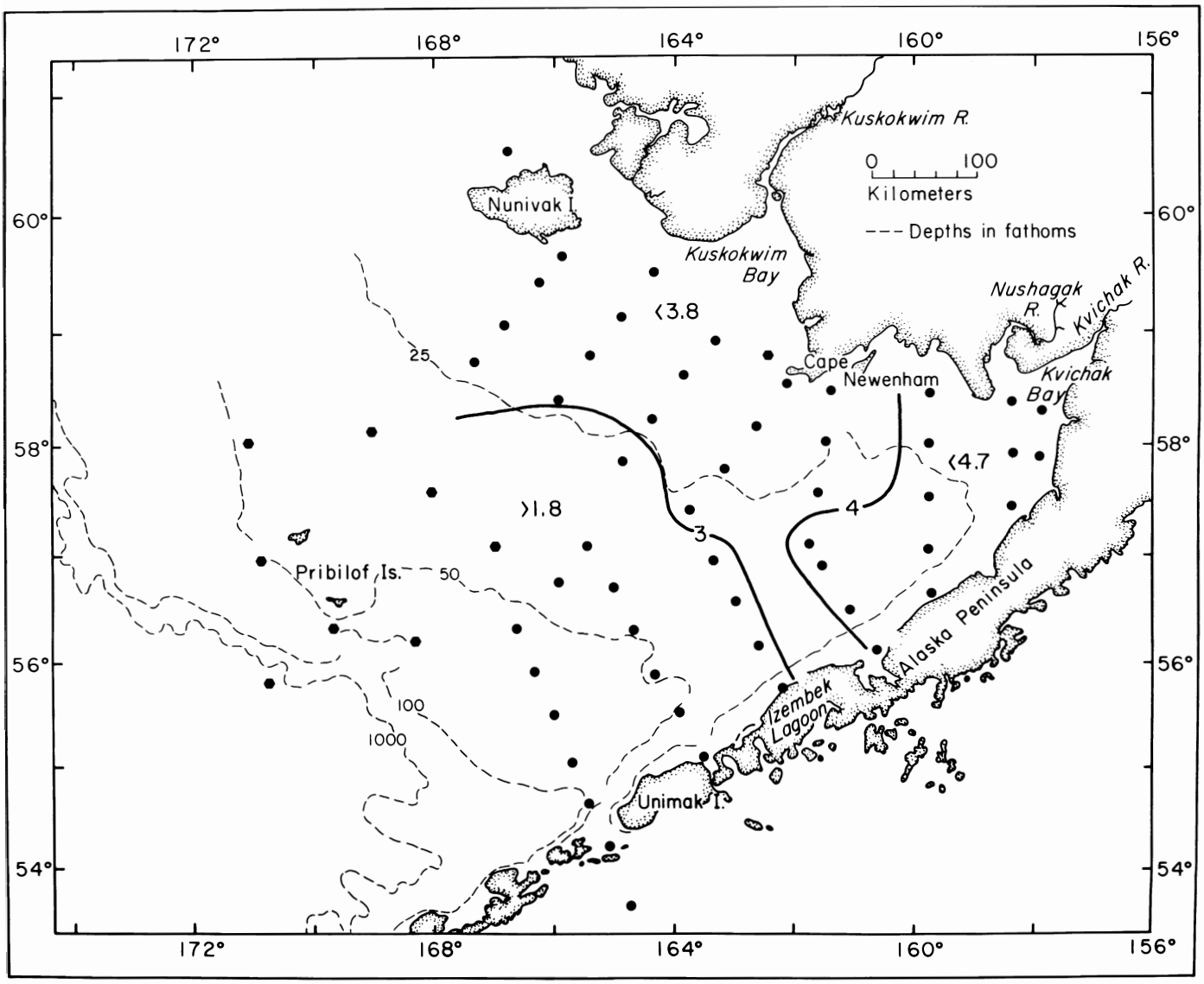

Figure 27-7. Surface distribution of dissolved ethene (nl/l, STP) in July 1976.

DISCUSSION

Source-Composition Relationships

Low molecular weight aliphatic hydrocarbons are ubiquitous in the surface waters of the world oceans (Swinnerton and Lamontagne 1974). Methane, the most abundant hydrocarbon, is generally at or near saturation in offshore surface waters, increasing in concentration in coastal and estuarine waters (Swinnerton and Lamontage 1974, Brooks and Sackett 1973, Scranton and Farrington 1977). Supersaturation of methane in coastal waters is largely attributed to methanogenesis occurring in bottom sediments (Oremland 1975), or similar processes occurring within suitable microenvironments (e.g., zooplankton, fecal matter, etc.) in the water column (Scranton and Farrington 1977). In localized areas of the Gulf Coast, gas seeps, underwater gas venting, and production activities associated with gas and oil development have led to significant enrichments of both methane and its natural saturated homologs in the water column (Brooks and Sackett 1973, Bernard et. al 1976, Brooks and Sackett 1977).

The source of C_{2+} hydrocarbons in pristine marine waters is not well understood. Our work in the coastal waters of Alaska clearly demonstrates that ethane, ethene, propane, and propene are limited to surface and shelf waters. Vertical profiles taken in the Alaskan Trench showed a rapid decrease in the concentrations of these hydrocarbons below 200 m. These observations and those of others (Swinnerton and Lamontagne 1974, Brooks and Sackett 1977) seem to indicate that the higher homologs of methane, including the alkenes, are derived from biological activity or perhaps photochemical reactions involving organic precursors in surface waters (R. Zika, Univ. of Miami, personal communication). These conclusions are supported by the laboratory studies of Wilson et al. (1970), and the *in-situ* observations of Swinnerton et al. (1977). In the latter report, correlations were observed between hydrocarbon production, light intensity, dissolved organic carbon, and chlorophyll *a*.

To effectively distinguish petroleum-derived hydrocarbons from biologically produced components, compositional or isotopic (^{14}C, ^{13}C) patterns must be characterized. One of the objectives of this report is to suggest several characteristic compositional patterns that might be useful in identifying the source of hydrocarbons. One such parameter is the ratio of methane to ethane plus propane (Brooks and Sackett 1973). The other, which will be developed here, is the ethane/ethene ratio. These two hydrocarbon species are particularly useful in a diagnostic sense because ethene is abundant in biological systems and absent in thermogenic sources. Conversely, ethane is relatively abundant in natural gas and petroleum.

In Fig. 27-8 the relationship between ethane (C_2) and ethene ($C_{2:1}$) is shown in two distinct hydrographic domains of Bristol Bay during July 1976. The relationship between ethane and ethene in surface waters (open circles) is shown by line (b). Linear regression of the observations yields the equation:

$$[C_2] = 0.28[C_{2:1}] - 0.20 \quad (r = 0.79).$$

Analyses made within 5 m of the bottom (solid circles) in the middle shelf domain also plot along this line, suggesting a common mechanism. In July, the water column was vertically stratified and rather turbid (Feely and Cline 1977); thus it is expected that photochemical reactions in the surface layers would have little effect on the distribution of hydrocarbons at depth.

As the deeper waters of St. George Basin are approached, the concentration of ethane increases relative to that of ethene (Fig. 27-8; line (a)). The equation of this line is:

$$[C_2] = 0.36[C_{2:1}] + 0.54 \quad (r = 0.88),$$

which reflects a higher production rate of ethane than of ethene. For comparative purposes, surface concentrations of ethane and ethene from Unimak Pass and waters near Izembek Lagoon also plot along this line.

Surface and middle shelf domain waters show a characteristic relationship in the relative abundances of ethane and ethene. In general, the concentration of ethene exceeds that of ethane by a factor of three

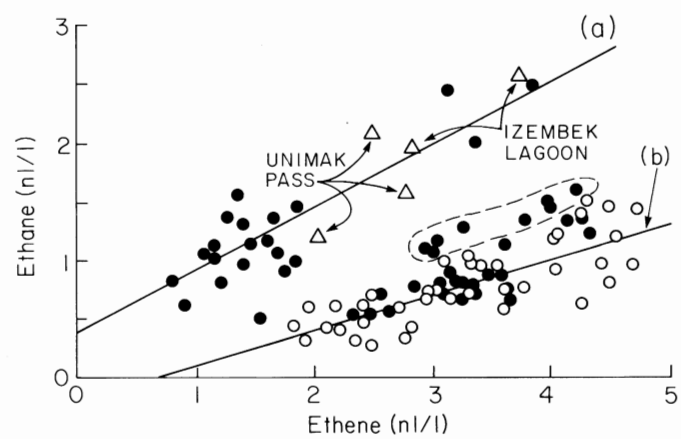

Figure 27-8. Relationship between the concentration of ethane and ethene for surface waters (open circles) and near-bottom waters (solid circles). Surface and near-bottom waters in the middle shelf region plot along line (b), whereas bottom waters from St. George Basin fall along curve (a). Surface waters from Unimak Pass and Izembek Lagoon also fall along curve (a). Transitional waters between St. George Basin and the middle shelf are outlined by the dashed line.

in well-oxygenated surface waters, like most Alaskan shelf areas studied (Cline et al. 1978). In the deeper water of St. George Basin (z > 100 m), the increase in the concentration of ethane is presumably related to the increased carbon flux to the sediments (Sharma 1979) and a concomitant drop in redox potential. Decaying plankton lying on the bottom (R. Reeburgh, Univ. of Alaska, personal communication) would be expected to give rise to an anoxic stratum at the bottom. This condition would favor increased production of ethane as was shown to occur in the anoxic waters of the Black Sea (Hunt 1974). It is not proposed that the near-bottom waters of St. George Basin are anoxic, only that microenvironments or microstrata near the bottom represent a significant source of ethane to the water column. Because the sediments of Izembek Lagoon are rich in organic matter (Barsdate et al. 1974), and are presumably anoxic, it is not surprising to find elevated concentrations of ethane near the entrance of the lagoon.

The relatively high concentrations of ethane found in the surface waters of Unimak Pass are the result of strong vertical mixing from below, but the possible influence of shipping, fishing, and transportation activities on the hydrocarbon distribution cannot be assessed at the present time.

As stated previously, hydrocarbons of different sources reflect distinct compositional patterns. Gaseous hydrocarbons generated in well-oxygenated waters or from shallow horizons in bottom sediments are usually characterized by high concentrations of methane (Brooks and Sackett 1973) and relatively high concentrations of alkenes (Bernard et al. 1978). Hydrocarbons derived from thermal processes are characteristically enriched in C_{2+} alkanes relative to methane and devoid of the alkenes (Frank et al. 1970, Clark and Brown 1977). Frank et al. (1970) have used these compositional characteristics to propose the ratio $[C_1]/[C_2]+[C_3]$ as a possible indicator of a source. Ratios in excess of 500 suggest a biological source, while ratios less than 50 indicate a thermogenic origin.

In an attempt to elucidate the origin of gaseous hydrocarbons, the ethane/ethene $[C_2]/[C_{2:1}]$ ratio was plotted against the methane/ethane plus propane $[C_1]/[C_2]+[C_3]$ ratio. Fig. 27-9 shows such a plot for distributions in Bristol Bay and includes two contrasting marine environments. Comparisons are made with the hydrocarbon distributions in the vicinity of the Norton Sound gas seep (Cline and Holmes 1977) and with the anoxic waters of the Black Sea (Hunt 1974). Including all the analyses from Bristol Bay, the $[C_1]/[C_2]+[C_3]$ ratio ranges from 30 to 500, while the $[C_2]/[C_{2:1}]$ ratio ranges between 0.1 and

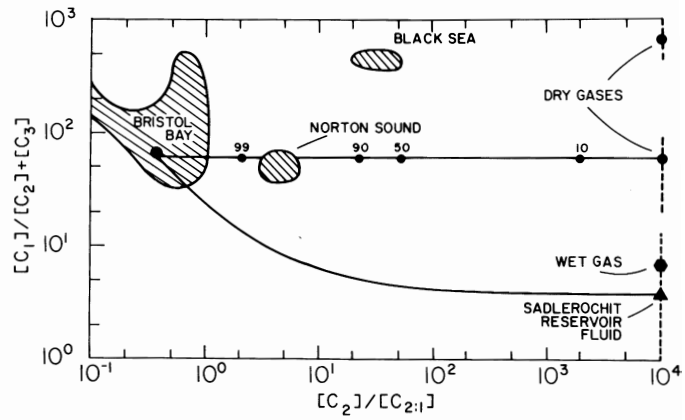

Figure 27-9. Compositional hydrocarbon trajectory diagram for Bristol Bay. For comparison, the compositional fields of the Norton Sound gas seep (Cline and Holmes 1977) and the anoxic waters of the Black Sea (Hunt 1974) are indicated. Mixing of Bristol Bay hydrocarbons with various thermogenically derived hydrocarbon mixtures results in a family of mixing trajectories, two of which are shown here (see text). Along one of the dry gas trajectories, the fraction (%) of ambient water is given, assuming that the hydrocarbons in the source are each about 100 times the ambient levels.

1. These compositional ratios obtain for most of the Alaskan shelf waters and are probably typical of high latitude, pristine coastal waters. On the other hand, anoxic waters in the Black Sea (Hunt 1974) reflect a narrow compositional field characterized by high concentrations of methane, $[C_1]/[C_2]+[C_3] \cong 500$, and relatively high concentrations of ethane, $20 < [C_2]/[C_{2:1}] < 50$. Provisionally, it is assumed that the Black Sea represents a model of the hydrocarbon composition to be expected from anoxic marine sources.

At this point it becomes useful to consider the compositional trajectories that might be observed if gases of thermogenic origin were mixed with biologically derived hydrocarbons. To accomplish this, four distinct petroleum/natural gas sources were considered from an analysis of gas and oil well data (Moore et al. 1966). The equations that govern the mixing trajectories in the $[C_1]/[C_2] + [C_3]$ and $[C_2]/[C_{2:1}]$ plane are:

$$\frac{[C_1]}{[C_2]+[C_3]} = \frac{[C_1]_A + ((1-x)/x)[C_1]_T}{[C_2]_A + [C_3]_A + ((1-x)/x)[C_2]_T + [C_3]_T} \quad (1)$$

$$\frac{[C_2]}{[C_{2:1}]} = \frac{[C_2]_A}{[C_{2:1}]_A} + ((1-x)/x)\frac{[C_2]_T}{[C_{2:1}]_A} \quad (2)$$

The fraction of ambient water is x, whereas concentrations of the individual hydrocarbons are shown in brackets. The two sources, between which mixing

is assumed to occur, are indicated by the subscripts A (ambient) and T (thermogenic source). The implicit assumptions are that the source ratios are constant and that the concentration of ethene in the natural gas source is zero.

To develop possible mixing scenarios, it was necessary to evaluate the possible range of LMW hydrocarbon mixtures that might occur as the result of offshore production. The $[C_1]/[C_2]+[C_3]$ frequency diagram for 366 terrestrial gas wells (Moore et al. 1966) was plotted, and by this means three discrete compositions, identified on the basis of their $[C_1]/[C_2]+[C_3]$ ratio, were defined, ranging from what is described as a "very" dry gas (methane rich) to a "typical" wet gas (methane poor). Some of the wet gases were associated with petroleum. A summary of the calculations is shown in Table 27-2.

TABLE 27-2.

Mean mole fraction of methane, ethane, and propane, calculated for three arbitrarily defined natural gas fractions (Moore et al. 1966). Number of samples used in each statistic calculation is shown in column 5. Standard deviation about the mean is shown in parentheses.

Mole Fraction			$\frac{[C_1]}{[C_2]+[C_3]}$		
C_1	C_2	C_3		n	Definition
.79(.11)	.075(.04)	.033(.026)	7	313	Wet Gas
.96(.02)	.011(.005)	.002(.002)	61	47	Dry Gas
.98(.02)	.001(.0006)	Tr	672	6	"Very" Dry Gas

The actual concentration ratio observed in the water will depend on the component partial pressure (or mole fraction), the Bunsen coefficient, which depends upon salinity and temperature, and the depth of water at which gas injection occurs. Implicit in the previous statement is that equilibrium is achieved between the gaseous and aqueous phases and that the rate of solution of the gases is a function of the thickness of the stagnant film boundary layer (Broecker and Peng 1974). Actually, equilibrium is probably not achieved. However, because the Bunsen coefficients and diffusion coefficients are similar for methane, ethane, and propane, the solubility ratio will not be significantly different from the equilibrium ratio. If these minimum conditions hold, the following expression relates the component partial pressure in the gas phase to the equilibrium solubility ratio:

$$\frac{[C_1]'}{[C_2]' + [C_3]'} = \frac{\beta_1 D_1 p_1}{\beta_2 D_2 p_2 + \beta_3 D_3 p_3} \qquad (3)$$

where β_i, D_i, and p_i represent the Bunsen coefficient, diffusion coefficient, and mole fraction of (1) methane, (2) ethane, and (3) propane. Assuming a mean temperature and salinity of 5 C and 30°/oo,

$D_1 = 0.85 \times 10^5$ cm^2/sec $\quad \beta_1 = 0.04$ ml CH_4 (STP)/ml H_2O
$D_2 = 0.69 \times 10^5$ cm^2/sec $\quad \beta_2 = 0.06$ ml C_2H_6 (STP)/ml H_2O
$D_3 = 0.55 \times 10^5$ cm^2/sec $\quad \beta_3 = 0.06$ ml C_3H_8 (STP)/ml H_2O

Bunsen coefficients (β_i), corrected for the "salting out effect" and the molecular diffusion coefficients (D_i), not corrected for the ionic strength of seawater, were estimated from the data of Bonoli and Witherspoon (1968). The solubility ratio, $[C_1]'/[C_2]'+[C_3]'$, for gas well data calculated from equation 3, is shown in Table 27-2 and is also shown as mixing end members in Fig. 27-9. Because it has been assumed that the concentration of ethene is zero (i.e., $[C_2]'/[C_{2:1}]' \rightarrow \infty$), the mixing end members are located at the extreme right margin.

The remaining end member we wish to consider is a wet gas associated with petroleum. For this purpose, the volatile fraction from the reservoir fluid of the Sadlerochit formation, Prudhoe Bay, was selected (Anon. 1971). The so-called volatile fraction, C_1 to C_4 hydrocarbons plus air gases, was normalized to 100 percent and the partial pressures of methane, ethane, and propane were calculated. As in the example given earlier, a gas of this composition is equilibrated with a parcel of Bristol Bay water. Table 27-3 gives the mole fraction composition of the gas phase and the resulting equilibrium solubility ratio. Bunsen coefficients and diffusion coefficients were the same as before.

TABLE 27-3.

Mole fractions of methane, ethane, and propane from the reservoir fluid of the Sadlerochit formation, Prudhoe Bay (Anon. 1971), and the resulting equilibrium solubility ratio. Gas phase was assumed to contain only C_1-C_4 hydrocarbons, nitrogen, carbon dioxide, and helium.

Mole Fraction			
C_1	C_2	C_3	$[C_1]'/[C_2]'+[C_3]'$
0.44	0.051	0.030	3.7

As expected, the gas is relatively rich in C_{2+} hydrocarbons and its composition is similar to that calculated earlier for a wet gas derived from gas wells. Of the gases present in the normalized mixture, methane, ethane, and propane constituted 81.6 percent by vol-

ume, C_4 hydrocarbons amounted to 3.4 percent, CO_2 was 14.2 percent, and the remaining 0.7 percent was divided between N_2 and He. Having estimated some possible petroleum and natural gas end members, trajectories that would result from mixing these end members with Bristol Bay water can be examined. The mixing trajectory resulting from the injection of a typical dry gas will be considered first.

To simplify the calculation, it is assumed that ambient Bering Sea water contains approximately the following concentrations of LMW alkanes: $[C_1]$ = 100 nl/l, $[C_2]$ = 1 nl/l, $[C_{2:1}]$ = 3 nl/l, and $[C_3]$ = 0.4 nl/l, giving a $[C_1]/[C_2]+[C_3]$ ratio of 71 and a $[C_2]/[C_{2:1}]$ ratio of approximately 0.33. It is apparent that this locus may be biased toward low values of the $[C_1]/[C_2]+[C_3]$ ratio (Fig. 27-9). If we assume that the local source of hydrocarbons is 100 times the ambient levels, the resulting mixing trajectory, computed from equations 1 and 2, is shown in Fig. 27-9. The values above the solid circles represent the percentage of ambient water at those points. Mixing a gas of this composition with the ambient water results in little change in the $[C_1]/[C_2]+[C_3]$ ratio, but a large shift in the $[C_2]/[C_{2:1}]$ ratio. This results directly from the assumption that the concentration of ethene was zero in the natural gas source. It is interesting that the mixing line passes through the compositional field observed in the region of the Norton Sound gas seep (Cline and Holmes 1977). Conclusions as to the source of thermogenic hydrocarbon gases in Norton Sound on the basis of this diagram would be misleading, however, since the ambient $[C_1]/[C_2]+[C_3]$ ratio in Norton Sound is significantly higher (~500) than the average value assigned for Bristol Bay (~71).

One additional feature of the compositional field diagram (Fig. 27-9) is that the mixing line between two defined sources is invariant with respect to the source concentrations of the hydrocarbons, as long as the ratios are fixed. This means that regardless of the source strength, compositional changes due to mixing will occur along the mixing line between the two sources. With the relative concentrations (i.e., 100:1) chosen in the above example, seepage or leakage of a dry gas in Bristol Bay would be observable to approximately 99 percent dilution. If the relative concentration ratio is increased to 1000:1, the effect is observable to 99.9 percent dilution.

Finally, we calculate the hypothetical mixing line, assuming a wet gas composition similar to that found in the Sadlerochit formation. This trajectory is also reflected in Fig. 27-9 and lies significantly below the previously calculated dry gas curve.

General conclusions drawn from Fig. 27-9 are that typical wet and dry gases should be readily distinguishable from biologically produced hydrocarbons using a combination of the $[C_1]/[C_2]+[C_3]$ and $[C_2]/[C_{2:1}]$ ratios. The composition of LMW hydrocarbon mixtures characterized by $[C_1]/[C_2]+[C_3] < 20$ and $[C_2]/[C_{2:1}] > 100$ strongly suggests that they are thermally derived. The exception is a methane-rich dry gas, such as that produced currently from several wells in upper Cook Inlet (Kelly 1968). These gas wells contain methane in excess of 98 mole percent, only traces of ethane, and no measurable propane. An injected gas of this composition, in all likelihood, will not be distinguishable from the suite of hydrocarbons formed biologically under anoxic conditions (e.g., in sediments, lagoon environments, anoxic waters). Consequently, a dry gas of this composition would be interpreted as biogenic on the basis of its $[C_1]/[C_2]+[C_3]$ and $[C_2]/[C_{2:1}]$ ratios.

Additional useful tracers include the $[C_2]/[C_3]$ ratio (Nikonov 1972) and the $\delta^{13}C$ composition of the seep methane (Brooks et al. 1974, Bernard et al. 1976). In the latter study, Bernard and coworkers have plotted the $\delta^{13}C$ of the dissolved methane against the $[C_1]/[C_2]+[C_3]$ ratio for a number of gas seeps investigated along the Texas shelf. Biogenic methane was found to be isotopically light ($-60^o/oo$ to $-70^o/oo$ vs. PDB), whereas methane derived from thermogenic sources was significantly heavier at $-40^o/oo$ to $-50^o/oo$. In a similar study, Kvenvolden et al. (1979) found the pore fluid methane at the locus of the seep in Norton Sound to be isotopically heavy at $-36^o/oo$, suggesting a thermal source.

There is no doubt that the isotopic composition of dissolved methane is an excellent diagnostic parameter in identifying the origin of natural gas. However, usually the concentration of methane is so low as to preclude the use of isotopic fingerprinting, except where gas venting is vigorous (e.g., Bernard et al. 1976). At low concentrations, the compositional ratios should be useful in identifying sources of hydrocarbons and their spatial trajectories. Because these hydrocarbons are dissolved, they readily identify the trajectories of other dissolved components, which may possess greater toxicity (e.g., benzene).

In the following discussion, attention will be given to the dispersion field of LMW hydrocarbons originating from a localized source and some estimates of the areal diffusion and advection scales applicable to Bristol Bay.

Dispersion model

The major advantages of using LMW hydrocarbons as *in-situ* tracers of petroleum are related to their relatively high abundance in crude oil and natural gas

and the low concentration levels at which they can be measured. In the event of a spill, well blowout, or subsurface seep, it becomes useful to define the trajectory and areal impact of the dissolved and suspended hydrocarbons. Because the LMW hydrocarbons are moderately soluble, these compounds become useful tracers of the soluble fraction. It is not the purpose of this report to model actual gas or oil seeps in Bristol Bay, since none were found, but rather to provide general guidelines on the usefulness of LMW hydrocarbons as tracers of the dissolved fractions of petroleum.

For simplicity we assume that the petroleum source is continuous and steady in time, and results in a vertically homogeneous distribution within a selected layer (e.g., surface mixed layer). The model describing these minimum conditions is a two-dimensional advection-diffusion equation given by Csanady (1973):

$$\frac{\partial}{\partial y}\left[K_y \frac{\partial c}{\partial y}\right] - U\frac{\partial c}{\partial x} - kC = 0, \qquad (4)$$

where C is the concentration of the dissolved hydrocarbon, x and y are space coordinates, K_y is the scale-dependent horizontal eddy diffusivity, U is the mean horizontal velocity in the x-direction, and k is a first-order decay constant. In this case, we will use the first-order decay term to describe the air-sea exchange process and assume biological oxidation and production to be negligible. Because the source of hydrocarbons is presumably small, the horizontal eddy diffusivity depends on the mixing scale (Okubo 1971). The solution to equation 4 for a line source is given by Csanady (1973) and is reproduced here without derivation:

$$\bar{C}(x,y) = \tfrac{1}{2}\bar{C}_o \exp(-kx/U)[\mathrm{erf}((L/2+y)/\sqrt{2\sigma_y}) + \mathrm{erf}((L/2-y)/\sqrt{2\sigma_y})] \qquad (5)$$

where $\bar{C}_o$ is the vertically integrated concentration at x = 0, L is the length of the line source, and σ_y is related to K_y through the equation $K_y = (U/2)(d\sigma_y{}^2/dx)$. Equation 5 is given in terms of the concentration at x = 0 rather than the production rate. This was done because the input rate for a seep would be difficult to quantify. Moreover, to our knowledge the production rate of known submarine gas seeps has never been documented. Thus, the model is expressed in terms of the concentration field, which should be easily measured. To simplify the discussion in terms of maximum trajectory scales, only the centerline distributions (y = 0) will be discussed. Hence:

$$\bar{C}(x,o) = \bar{C}_o \exp(-kx/U)[\mathrm{erf}(L/\sqrt{8\sigma_y})] \qquad (6)$$

Using empirical relationships presented by Okubo (1971), where $\sigma_{rc}^2 = 0.0108t^{2.34}$, U = x/t, and $\sigma_{rc}^2 = 2\sigma_x\sigma_y$, equation 6 becomes

$$\bar{C}(x,o) = \bar{C}_o \exp(-kx/U)[\mathrm{erf}(L/0.208(x/U)^{1.17})] \qquad (7)$$

after substitution.

In Bristol Bay, as in any body of water, the source of gas may be at the surface or at depth. To discuss dispersion scales under both these conditions we will assume that (1) the source is at the surface and is consequently influenced by air-sea exchange and (2) the source is at depth and physically isolated from the surface by a strong pycnocline (k = 0). We further assume that the component is biologically unreactive, which is a reasonable assumption at low concentrations. Methane will be selected as the model component but any of the LMW hydrocarbon species would suffice. Equation 5 is valid for all dissolved hydrocarbon species that possess chemical and biochemical reactivities similar to that of methane.

Under the assumptions of the model, methane injected at the surface will be dispersed by diffusion and advection, and lost from the system through air-sea transfer. The flux of methane across the air-sea boundary can be described by the stagnant film boundary layer model (Broecker and Peng 1974),

$$F_1 = (D/h)(\bar{C}_1 - C_1'), \qquad (8)$$

where D is the molecular diffusion coefficient, h is the thickness of the stagnant film, $\bar{C}_1$ is the average concentration in the mixed layer, and C_1' is the equilibrium solubility concentration. The thickness of the molecular film is a function of sea-surface roughness or wind velocity (Emerson 1975). From the derivation of Fick's second law, it can be readily shown that transport across the sea surface is:

$$T_1 = (D/\Delta z \cdot h)(\bar{C}_1 - C_1'), \qquad (9)$$

where Δz is the depth of the surface mixed layer. Thus from equation 9 and by analogy to equation 4:

$$k = D/\Delta z \cdot h. \qquad (10)$$

In order to assess the importance of air-sea exchange on the methane dispersion scale, the value of k must be estimated. To accomplish this, nominal seasonal values for surface temperature and mean sca-

lar surface winds were used. All other parameters were computed from these data. Parameters used in the calculation of k are summarized in Table 27-4.

TABLE 27-4

Parameters used in the estimation of the first order decay constant (equation 10) governing the escape rate of methane across the sea surface.

	Temp.[a] °C	Wind Speed[b] m/sec	D_1[c] cm²/sec	Δz[a] m	h[d] μm	k /sec
Summer	10	6.3±0.8	1.1×10^{-5}	20	80	6.6×10^{-7}
Winter	0	9.9±0.5	0.65×10^{-5}	75	15	5.8×10^{-7}

[a]Kinder and Schumacher, Chapter 4, this volume
[b]Brower et al., 1977
[c]Bonoli and Witherspoon, 1968
[d]Emerson, 1975

Mean monthly wind velocities were averaged for the months of May-August (summer) and November-February (winter). Diffusion coefficients were taken from the data presented by Bonoli and Witherspoon (1968) and corrected to 0.5M NaCl solutions according to their equation. Thickness of the molecular film as a function of wind velocity was read from the graph presented by Emerson (1975). Because the effects of sea-surface roughness on the stagnant film thickness (h) and mixed layer depth on the rate constant (k) are seasonally compensating, a mean value of 6.2×10^7/sec was adopted in the calculation (Table 27-4). For comparison, this value is approximately one-half the value calculated for the surface waters of Walvis Bay by Scranton and Farrington (1977).

The solution of equation 7 requires that an appropriate source dimension (L) and mean velocities (U) be chosen. Equation 7 is the solution for a line source of length L; however for our purpose here, we will assume that the source is distributed along L rather than an extended point source. The results are equivalent at distances greater than 10 L (personal communication, J. Lavelle, PMEL). The length of the source was set arbitrarily at 1 km, which is probably appropriate for a surface spill, but would be excessive for small subsurface seeps.

Current trajectories and mean current velocities for Bristol Bay are known (Kinder and Schumacher, Chapter 5, this volume). Typical values for the middle shelf are 2 cm/sec, whereas velocities near the slope are in the neighborhood of 10 cm/sec. These values were selected for simulation of the dispersion field, although velocities greater than 10 cm/sec may occur during storms (Kinder and Schumacher, Chapter 5, this volume). Of course, higher velocities are observed at tidal frequencies, but this effect is included as diffusive transport in equation 4 (Coachman and Charnell 1979).

The results of the simulation are reflected in Fig. 27-10 for the assumed velocity fields. Dashed lines show the centerline normalized concentration of methane in the absence of air-sea evasion (k=0). If it is assumed that the input rate along L increased the local concentration of methane to a factor of 100 (C/C_o) above background (i.e., 10,000 nl/l), methane could be observed down the axis of flow for a distance of 150 km in the surface layers and 400 km in the bottom waters, assuming a mean current flow of 10 cm/sec. Actual trajectory scale in the surface waters will probably be somewhat greater, because the air-sea transfer rate is proportional to the term $(\bar{C}_1 - C_1')$ (see equation 9). In effect, the transfer rate decreases as the concentration of methane in the

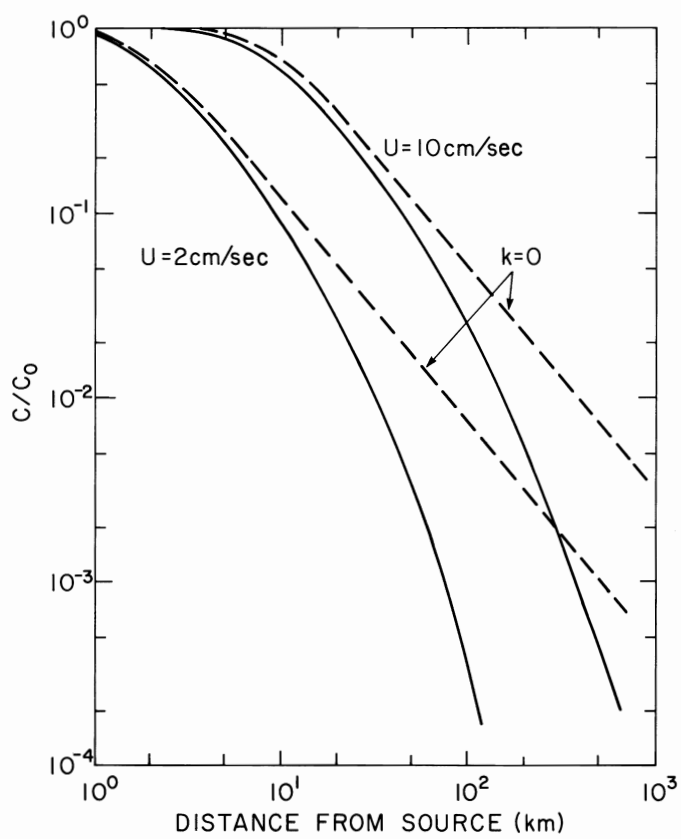

Figure 27-10. Relative decrease in the concentration of a dissolved hydrocarbon from a line source 1 km in diameter as estimated by a steady-state, horizontal diffusion/advection model. Surface ($k = 6.2 \times 10^7$/sec) and near-bottom trajectories (k = 0) are considered for mean flows of 2 cm/sec and 10 cm/sec.

plume approaches the saturation value; in this case the equilibrium concentration would be approximately 50 nl/l. At reduced mean current velocities, lateral diffusion becomes more important, reducing the concentration of methane along the axis of the plume. At velocities of only 2 cm/sec, methane would be observable along the centerline of the plume for distances of 40 km and 80 km, depending on whether the injection was at the surface or at depth (k = 0). Clearly, small seeps can be traced for considerable distances, particularly if the injection occurs at depth, where hydrostatic pressure increases the local concentration.

At this point, it becomes pertinent to ask what hydrocarbon enrichment might be expected from a gas seep, natural or otherwise. A typical wet gas, as described earlier (Fig. 27-9), might be expected to contain mole fractions of methane, ethane, and propane of 0.80, 0.075, and 0.033 respectively. Assuming that the injection of a gas of this composition occurred at 50 m (ca. 5 atm hydrostatic pressure) and that the water column became saturated locally with respect to each of these gases, concentrations of methane, ethane, and propane would reach saturation values of 1.8×10^8 nl/l, 2.5×10^7 nl/l, and 1.0×10^7 nl/l, respectively. (It has been assumed that the effect of hydrostatic pressure on solubility is linear.) Assuming ambient levels of methane, ethane, and propane of 200 nl/l, 2 nl/l, and 1 nl/l (these values are about twice the actual mean values for the middle shelf region; see Table 27-1), the enrichment factors for methane, ethane, and propane become 1.0×10^6, 1.2×10^7, and 1.0×10^7, respectively. Assuming that the injection of gas was at 50 m as above, these hydrocarbons would be observable along the axis of the plume for distances up to 1,000 km. Here a signal-to-noise ratio of approximately two is assumed. Actual longitudinal trajectories will depend on a number of factors: the scale of the seep, mean current velocities, diffusivity near the source, and biological oxidation processes in the water and at the surface of the sediments. Biological oxidation is likely to be much more important at the higher concentrations of hydrocarbons, thereby reducing the trajectory scale. Even in the surface layer, we estimate that LMW hydrocarbons could be traced for several hundreds of kilometers, depending on a number of factors. Among these are the state of the surface microlayer (wind velocity, surface organics, etc.), depth of the mixed layer (vertical dilution), microbial oxidation, and the mean current velocity.

While the above calculations are crude, they nevertheless serve to delineate the usefulness of LMW hydrocarbons as effective tracers over moderate space scales. In the Norton Sound gas seep (Cline and Holmes 1977), the ethane plume was observable for at least 140 km downstream of the source for a source enrichment of about 20 above ambient. Referring to Fig. 27-10, and assuming a 2 cm/sec mean current velocity near the bottom (Muench et al., Chapter 6, this volume), the model predicts a longitudinal trajectory scale of 100 km (k=0). In this case, the model appears to underestimate the actual observed scale, possibly by as much as a factor of two. The reasons for the disparity are numerous; among them are variable gas seepage rate, fluctuating currents, inappropriate near-source diffusive scale, and poor characterization of the dimension of the ethane source. Given the hydrographic uncertainties and model assumptions, the prediction is probably as good as can be developed at this time.

SUMMARY

The concentrations of dissolved LMW hydrocarbons in Bristol Bay are relatively low when compared with other Alaskan shelf waters. Methane, the most abundant hydrocarbon, is near saturation concentration in surface waters, but increases significantly near lagoons along the Alaska Peninsula. There appears to be no major production of methane from the bottom sediments of the middle shelf but significant amounts are produced seasonally from the organic-rich sediments of St. George Basin. The distribution of methane is largely controlled by mean flow and frontal dynamics.

The C_{2+} fraction shows seasonal variability and appears to be regulated by biological processes, presumably microorganisms. As observed elsewhere in Alaskan coastal waters, the alkenes are more abundant than the alkanes of the same carbon number. The concentration of ethane, for example, has a linear relation to the concentration of ethene, which suggests a common precursor or source. Low concentrations of LMW hydrocarbons, a relatively high $[C_1]/[C_2]+[C_3]$ ratio of 30 to 500, and a $[C_2]/[C_{2:1}]$ ratio of less than 1.0, all suggest a biological source. Since no evidence was found in the LMW hydrocarbon fraction for the presence of petroleum-like hydrocarbons, we conclude that Bristol Bay is pristine.

Comparison of the hydrocarbon composition of typical natural gas and petroleum with those found in Bristol Bay shows that small amounts of thermogenically derived gases should be readily discernible in the water column, depending, of course, on the magnitude of the source. On the basis of the $[C_1]/[C_2]+[C_3]$ and $[C_2]/[C_{2:1}]$ ratios, a thermogenic

field applicable to Bristol Bay can be defined. In general, $[C_1]/[C_2]+[C_3]$ ratios less than 20 and $[C_2]/[C_{2:1}]$ ratios greater than 100 strongly suggest a thermogenic source. A very dry natural gas (CH_4 > 98 mole percent), similar to that currently being produced in Cook Inlet, represents an exception to the foregoing generalizations. In all likelihood, a methane-rich gas of thermogenic origin would appear to be of biological origin in the $[C_1]/[C_2]+[C_3]$ and $[C_2]/[C_{2:1}]$ compositional fields.

Finally, an estimate was made of the possible dispersion scale of LMW hydrocarbons arising from a line source, using a steady-state two-dimensional model. On the basis of typical mean velocities of 2 and 10 cm/sec with the inclusion of a sink term for air-sea exchange, it was estimated that dissolved LMW hydrocarbons would be identifiable in surface waters over distances of 40-150 km, assuming a local hydrocarbon concentration of 100:1 above ambient. At depth below a strong pycnocline, the horizontal mixing scale increases to 100-500 km. Actual trajectory scales expected in Bristol Bay will depend on a number of factors. Among them are the strength of the source, degree of solution, diffusive mixing scales, air-sea exchange, and biological oxidation rates.

In this report the usefulness of LMW hydrocarbons as a diagnostic indicator of petroleum hydrocarbon is described. Not only are these gases excellent tracers of dissolved or emulsified petroleum hydrocarbons, but their ease of measurement allows real-time observations to be made—a valuable adjunct to a monitoring program.

ACKNOWLEDGMENTS

I wish to thank Lee Ohler, Anthony Young, and Susan Hamilton, who participated in the cruises to the Bering Sea. Special thanks are due to Charles Katz, who diligently scrutinized the data for errors and organized it into a usable form. Criticism of the manuscript was provided by Drs. H. Curl, R. Feely, J. Lavelle, and J. Schumacher of PMEL/NOAA, Dr. K. Kvenvolden of USGS, and Dr. R. Gammon of the University of Washington. To all these people I am grateful for their helpful suggestions. Finally, I wish to express gratitude to the captains and crews of the NOAA research ships *Discoverer* and R/V *Moana Wave*, without whose assistance in the field this work could not have been carried out.

This study, Contribution No. 456 from the NOAA/ERL Pacific Marine Laboratory, was supported by the Bureau of Land Management through interagency agreement with the National Oceanic and Atmospheric Administration, under which a multiyear program responding to the needs of petroleum development of the Alaskan shelf is managed by the Outer Continental Shelf Environmental Assessment Program (OCSEAP) Office.

REFERENCES

Anonymous
1971 Prudhoe Bay data are revealed at Alaska for the first time. Gas and Oil J., 57-64.

Barsdate, R. J., M. Nebert, and C. P. McRoy
1974 Lagoon contributions to sediments and water of the Bering Sea. *In:* Oceanography of the Bering Sea, D.W. Hood and E.J. Kelley, eds., 553-78. Inst. Mar. Sci., Occ. Pub. No. 2, Univ. Alaska, Fairbanks.

Bernard, B. B., J. M. Brooks, and W. M. Sackett
1976 Natural gas seepage in the Gulf of Mexico. Earth Planet. Sci. Lett. 31: 48-54.

1978 Light hydrocarbons in recent Texas continental shelf and slope sediments. J. Geophys. Res. 83: 4053-61.

Bonoli, L., and P. A. Witherspoon
1968 Diffusion of paraffin, cycloparaffin and aromatic hydrocarbons in water and some effects of salt concentration. *In:* Advances in organic chemistry, P.A. Schenck and I. Havenaar, eds., 373-84. Pergamon Press, New York.

Broecker, W. S., and T. H. Peng
1974 Gas exchange rates between air and sea. Tellus 26: 21-35.

Brooks, J. M., J. R. Gormly, and W. M. Sackett
1974 Molecular and isotopic composition of two seep gases from the Gulf of Mexico. Geophys. Res. Lett. 1: 213-16.

Brooks, J. M., and W. M. Sackett
1973 Sources, sinks, and concentrations of light hydrocarbons in the Gulf of Mexico. J. Geophys. Res. 78: 5124-58.

1977 Significance of low-molecular-weight hydrocarbons in marine waters. *In:* Proc. 7th Inter. Meeting on Organic Geochemistry. 455-68.

Brower, W. A., Jr., H. W. Searby, J. L. Wise, H. F. Diaz, and A. S. Prechtel
1977 Climatic atlas of the outer continental shelf waters and coastal regions of Alaska: II, Bering Sea. AEIDC, Univ. Alaska, Anchorage.

Carlisle, C. T., G. S. Bayliss, and D. G. Vandelinder
1975 Distribution of light hydrocarbons in seafloor sediments: Correlations between geochemistry, seismic structure, and possible reservoired oil and gas. OTC 2341: 65-8.

Clark, R. C., and D. W. Brown
1977 Petroleum: Properties and analyses in biotic and abiotic systems. *In:* Effects of petroleum on Arctic and Subarctic marine environments and organisms, 1-90. Academic Press, N.Y.

Cline, J.D.
1977 Distribution of light hydrocarbons, C_1-C_4, in the northeast Gulf of Alaska, Lower Cook Inlet, southeastern Chukchi Sea. *In:* Environmental assessment of the Alaskan continental shelf, 8: 180-268. DOC/NOAA.

Cline, J. D., and R. Feely
1976 Distribution of light hydrocarbons, C_1-C_4, in the Gulf of Alaska and southeastern Bering Shelf. *In:* Environmental assessment of the Alaskan continental shelf, 9: 443-547. DOC/NOAA.

Cline, J. D., R. Feely, and A. Young
1978 Identification of natural and anthropogenic petroleum sources in the Alaskan shelf areas utilizing low molecular weight hydrocarbons. *In:* Environmental assessment of the Alaskan continental shelf, 8: 73-198, DOC/ NOAA.

Cline, J. D., and M. L. Holmes
1977 Submarine seepage of natural gas in Norton Sound, Alaska. Science 198: 1149-53.

Coachman, L. K., and R. L. Charnell
1977 Finestructure in outer Bristol Bay, Alaska. Deep-Sea Res. 24: 869-89.

1979 On lateral water mass interaction—A case study, Bristol Bay, Alaska. J. Phys. Oceanogr. 9: 278-97.

Csanady, G. T.
1973 Turbulent diffusion in the environment. D. Reidel Publishing, Boston.

DOI/DOC (Department of the Interior/Department of Commerce)
1975 Environmental assessment of the Gulf of Alaska, Southeastern Bering and Beaufort Seas, Boulder, Colo.

Dunlap, H. F., J. S. Bradley, and T. F. Moore
1960 Marine seep detection—A new reconnaissance exploration method. Geophysics 25:275-82.

Ehhalt, D. H.
1974 The atmospheric cycle of methane. Tellus 26: 58-70.

Emerson, S.
1975 Gas exchange rates in small Canadian Shield lakes. Limnol. Oceanogr. 20: 754-61.

Feely, R., and J. D. Cline
1977 The distribution, composition, and transport of suspended particulate matter in the northeastern Gulf of Alaska, southeastern Bering shelf, and lower Cook Inlet. *In:* Environmental assessment of the Alaskan continental shelf, 8: 89-179, DOC/ NOAA.

Frank, D. J., W. M. Sackett, R. Hall, and A. D. Fredericks
1970 Methane, ethane, and propane concentrations in the Gulf of Mexico. Amer. Assoc. Petrol. Geol. Bull. 54: 1933-8.

Harrison, H., J. E. Johnson, and J. D. Cline
1980 Light hydrocarbons in the atmospheric boundary layer over the North Pacific. (Submitted to J. Geophys. Res.)

Hunt, J. M.
1974 Hydrochemistry of Black Sea. *In:* The Black Sea, geology, chemistry, and biology, E.T. Degens and D.A. Ross, eds., 499-504. Amer. Assoc. Petrol.Geol. Mem. 20.

Kelly, T. E.
1968 Gas accumulations in non-marine strata, Cook Inlet, Basin, Alaska. *In:* Natural gases of North America, B.W. Beebe, ed., 49-64. Amer. Assoc. Petrol. Geol. Mem. 9, Part I.

Kinder, T. H.
1977 The hydrographic structure over the continental shelf near Bristol Bay, Alaska, June 1976. Dep. Oceanogr. Tech. Rep. M77-3: 1-61. Univ. of Washington.

Kinder, T. H., and L. K. Coachman
1978 The front overlying the continental slope in the eastern Bering Sea. J. Geophys. Res. 83: 4551-9.

Kvenvolden, K. A., K. Weliby, C. H. Nelson, and D. J. Desmarais
1979 Submarine carbon dioxide seep in Norton Sound, Alaska. Science 205: 1264-6.

Lamontagne, R. A., W. D. Smith, and J. W. Swinnerton
1975 C_1-C_3 hydrocarbons and chlorophyll *a* concentrations in the equatorial Pacific Ocean. *In:* Analytical methods in oceanography, T.R.P. Gibbs, Jr., ed., 163-71. Advances in Chemistry Series 147, Amer. Chem. Soc.

McCarty, P. L.
1964 The methane fermentation. *In:* Principles and applications in aquatic microbiology, H. Heukelekian and N.C. Dondero, eds., 314-43. John Wiley, N. Y.

Moore, B. J., R. D. Miller, and R. D. Schrewsbury
1966 Analyses of natural gases of the United States, 1964. Bureau of Mines IC-8302: 1-144.

Nikonov, V. F.
1972 Distribution of methane homologs in gas and oil fields. Doklady Akad. Nauk SSSR 226: 234-6.

Okubo, A.
1971 Oceanic diffusion diagrams. Deep-Sea Res. 18: 789-802.

Oremland, R. S.
1975 Methane production in shallow-water, tropical marine sediments. Appl. Microbiol. 30: 602-8.

Reeburgh, W. S., and D. T. Heggie
1977 Microbial methane consumption reactions and their effect on methane distributions in freshwater and marine environments. Limnol. Oceanogr. 22: 1-9.

Sackett, W. M.
1977 Use of hydrocarbon sniffing in offshore exploration. J. Geochem. Explor. 7: 243-54.

Schumacher, J. D., T. H. Kinder, D. H. Pashinski, and R. L. Charnell
1979 A structural front over the continental shelf of the eastern Bering Sea. J. Phys. Oceanogr. 9: 79-87.

Scranton, M. I., and P. G. Brewer
1977 Occurrence of methane in the near surface waters of the western subtropical North Atlantic. Deep-Sea Res. 24: 127-38.

Scranton, M. I., and J. W. Farrington
1977 Methane production in the waters off Walvis Bay. J. Geophys. Res. 82: 4947-53.

Sharma, G. D.
1979 The Alaskan shelf. Springer-Verlag, N. Y.

Smith, A. M., and R. J. Cook
1974 Implications of ethylene production by bacteria for biological balance of soil. Nature (London) 252: 703-5.

Swinnerton, J. W., and R. A. Lamontagne
1974 Oceanic distribution of low-molecular-weight hydrocarbons. Environ. Sci. and Technol. 8: 657-63.

Swinnerton, J. W., R. A. Lamontagne, and J. S. Hunt
1977 Field study of carbon monoxide and light hydrocarbons production related to natural biological processes, NRL Rep. 8099: 1-9.

Swinnerton, J. W., and V. J. Linnenbom
1967 Determination of the C_1 to C_4 hydrocarbons in seawater by gas chromatography. J. Chromatogr. Sci. 5: 570-3.

Wilson, D. F., J. W. Swinnerton, and R. A. Lamontagne
1970 Production of carbon monoxide and gaseous hydrocarbons in seawater: Relation to dissolved organic carbon. Sci. 168: 1577-9.

Wolfe, R. S.
1971 Microbial formation of methane. *In:* Advances in microbial physiology, A.H. Hose and J.F. Wilkinson, eds., 6: 107-46. Academic Press, N. Y.

Yamamoto, S., J. B. Alcauskas, and T. E. Grozier
1976 Solubility of methane in distilled water and seawater. J. Chem. Eng. Data 21: 78-80.